**PAPER**

Check for updates

# Efficient wastewater treatment and biomass co-production using energy microalgae to fix C, N, and P

Han Yuan,[ac] Pengxinyue Huang,[a] Jiang Yu, [ID] *[acd] Pu Wang,*[b] Hong Bin Jiang,[b] Yinying Jiang,[ac] Siwei Deng,[ae] Zhi Huang,[ac] Jie Yu[a] and Weiwei Zhu[a]

Distillery wastewater (DWW), characterized by high organic and nutrient loads, represents a significant environmental challenge, requiring effective and sustainable treatment solutions. This study investigates an innovative approach that integrates microalgae cultivation with DWW treatment for simultaneous bioremediation and biomass production, while also exploring carbon sequestration. We analyzed the growth characteristics, nutrient removal efficiency, protein accumulation, and ultrastructural changes of *Chlamydomonas reinhardtii* and *Scenedesmus dimorphus* under varying nitrogen-to-phosphorus (N/P) ratios in diluted DWW. Optimal nutrient removal and biomass accumulation were achieved at N/P concentrations of $46/11.5$ mg $L^{-1}$. *C. reinhardtii* showed particularly high nutrient removal rates, with significantly high removal rates for total nitrogen, total phosphorus, and chemical oxygen demand. *S. dimorphus*, under the same conditions, demonstrated exceptional protein accumulation and also effectively removed pollutants. Both species showed enhanced performance under these conditions, with microalgal cell organelles remaining structurally intact, and chloroplasts and thylakoid layers well-developed. The study also explored carbon sequestration potential using varying $CO_2$ concentrations, where *C. reinhardtii* exhibited enhanced biomass accumulation at 3000 ppm $CO_2$. This integrated approach offers an effective and economically feasible solution for distillery wastewater treatment, simultaneously enabling biomass production and carbon capture. The dual benefits of bioremediation and bioenergy generation position this technology as a promising pathway for sustainable resource management and environmental protection.

## 1. Introduction

With the rapid development of the brewing industry, distillery wastewater (DWW), characterized by its high pollution load and treatment difficulty, has become a significant environmental challenge.[1] DWW is acidic and contains high concentrations of chemical oxygen demand (COD), biological oxygen demand (BOD), heavy metals (HMs), and endocrine-disrupting chemicals (EDCs), as well as being rich in nutrients such as nitrogen and phosphorus.[2–5] If untreated DWW is discharged into the environment, it not only reduces sunlight penetration in water bodies, decreases dissolved oxygen (DO) levels, and lowers

photosynthetic efficiency but also triggers eutrophication and disrupts ecosystem balance.[6]

Physical and chemical methods, as traditional wastewater treatment approaches, offer rapid treatment but come with high costs and the potential for secondary pollution.[7–12] Microalgae technology has gained significant attention due to its low cost and high efficiency in removing nutrients, as well as its ability to facilitate biomass resource recovery for multiple uses.[13,14] For example, Li *et al.*[15] and Shrasti Vasistha *et al.*[16] demonstrated that using different algal species to treat DWW resulted in increased biomass production and improved nutrient removal efficiency. However, most research is limited to monoculture systems, and the advantages of mixed culture systems have yet to be fully explored.

Microalgae are photosynthetic autotrophic microorganisms. Due to their rapid growth, efficient photosynthesis, and diverse metabolites, they have garnered significant attention in wastewater treatment and bioenergy development.[17,18] Organic and inorganic pollutants in distillery wastewater (DWW) can serve as carbon sources and nutrients for microalgae, respectively. Combining microalgae cultivation with DWW treatment can significantly enhance the removal efficiency of nitrogen and

*[a]Department of Environmental Science and Engineering, College of Architecture and Environment, Sichuan University, Chengdu, 610065, PR China. E-mail: yuj@scu.edu.cn*

*[b]Suining Ecological Environmental Monitoring Centre of Sichuan Province, Suining Sichuan 629000, China*

*[c]Institute of New Energy and Low Carbon Technology, Sichuan University, Chengdu, 610065, PR China*

*[d]Yibin Institute of Industrial Technology, Sichuan University, Yibin 644000, PR China*

*[e]Soil and Groundwater Pollution Prevention Research Institute, Sichuan Academy of Eco-Environmental Sciences, 610046, Chengdu, P. R. China*

phosphorus while reducing cultivation costs.[19] Studies have shown that optimizing the nitrogen-to-phosphorus (N/P) ratio can markedly improve nutrient removal effectiveness.[20,21] Additionally, microalgae convert inorganic carbon into carbohydrates through photosynthesis and release $O_2$, creating a novel and efficient carbon sequestration model that has become a hot research topic in air pollution control.[22] The carbon content of microalgae is typically 0.5 kg C kg$^{-1}$ dry weight (DW), and their average carbon capture capacity is 1.8 kg $CO_2$ kg$^{-1}$ DW.[23] Furthermore, microalgae are 10 to 50 times more effective at carbon sequestration than terrestrial plants.[24] The $CO_2$ content in industrial flue gas can reach 10% to 30%, and using it as a carbon source for microalgae cultivation can not only lower cultivation costs but also achieve the dual goals of $CO_2$ fixation and environmental benefits.

In light of the insufficient focus on mixed cultures and the optimization of N/P concentrations in existing studies,[25] this research investigates *Chlamydomonas reinhardtii* and *Scenedesmus dimorphus*. The growth characteristics, nutrient removal, protein accumulation, and ultrastructural changes of these species were systematically examined at various N/P concentrations. Additionally, the study explores the carbon sequestration mechanism in relation to different concentrations of exogenous $CO_2$. The findings are expected to offer new insights for the treatment and resource utilization of distillery wastewater (DWW), while also achieving the comprehensive goals of efficient microalgal cultivation and high-value product extraction.

## 2. Methods and methods

### 2.1. Microalgae resources and wastewater components

*C. reinhardtii* and *S. dimorphus* were both obtained from the Algae Culture Laboratory at the College of Life Sciences, Sichuan University. These two microalgae strains were cultured in modified WC (Woods Hole Chu #10) medium, with potassium phosphate tribasic monohydrate ($K_2HPO_4 \cdot 3H_2O$) (1.55 mg P L$^{-1}$) and sodium nitrate ($NaNO_3$) (14 mg N L$^{-1}$) as phosphorus and nitrogen sources, respectively. Before the formal experiment began, the microalgae were first acclimated and cultured in WC medium to ensure that the microalgae were in the logarithmic growth phase. The composition of the WC medium is detailed in Table 1.

This study utilized distillery wastewater (DWW) from the Huangjia Baxian Distillery in Shuangliu County, Chengdu, Sichuan Province, which produces lager beer. Before microalgae cultivation, the DWW was first filtered through a 0.45 μm pore-sized cellulose acetate filter paper, then sterilized by autoclaving at 121 °C for 30 minutes, and stored sealed at 4 °C for later use. The composition of the DWW is shown in Table 2. The values presented in Table 3 for raw wastewater, after air floated, and after autoclaved, are all from the same sample, but are presented as a mean of 3 measurements.

Various dilution ratios of the DWW (undiluted: 100%, v/v; 2-fold: 50%, v/v; 4-fold: 25%, v/v; 8-fold: 12.5%, v/v) were tested. Preliminary experiments revealed that microalgae exhibited no growth in the undiluted wastewater medium due to the high

**Table 1** Composition of the modified WC medium

| S. No. | Components | Concentration (g L$^{-1}$) | Volume (mL) |
|---|---|---|---|
| 1 | $CaCl_2 \cdot 2H_2O$ | 1.165 | 1 |
| 2 | $MgSO_4 \cdot 7H_2O$ | 95.890 | 1 |
| 3 | $NaHCO_3$ | 14.162 | 1 |
| 4 | $K_2HPO_4 \cdot 3H_2O$ | 5.991 | 1 |
| 5 | $NaNO_3$ | 0.423 | 1 |
| 6 | Trace elements | | 1 |
| | $Na_2EDTA$ | 4.36 | |
| | $FeCl_3 \cdot 6H_2O$ | 3.15 | |
| | $CuSO_4 \cdot 5H_2O$ | 0.01 | |
| | $ZnSO_4 \cdot 7H_2O$ | 0.022 | |
| | $CoCl_2 \cdot 6H_2O$ | 0.01 | |
| | $MnCl_2 \cdot 4H_2O$ | 0.18 | |
| | $NaMoO_4$ | 0.006 | |
| | $H_3BO_{13}$ | 1.00 | |

**Table 2** Physicochemical characteristics of distillery wastewater (DWW) before and after pretreatment

| Parameters | Raw wastewater | After air floated | After autoclaved |
|---|---|---|---|
| pH | 3.62 | 6.92 | 6.87 |
| COD (mg L$^{-1}$) | 61 000 | 2021 | 1200 |
| TN (mg L$^{-1}$) | 2125 | 52 | 46 |
| TP (mg L$^{-1}$) | 592 | 13 | 11.5 |

**Table 3** $CO_2$ fixation rates of *C. reinhardtii* at different $CO_2$ concentrations

| $CO_2$ concentration (ppm) | Biomass productivity (mg L$^{-1}$ d$^{-1}$) | $CO_2$ fixation rate (mg L$^{-1}$ d$^{-1}$) |
|---|---|---|
| 380 | 27.02 | 44.59 |
| 3000 | 50.95 | 84.07 |
| 6000 | 7.98 | 13.16 |
| 9000 | 0.64 | 1.05 |

alcohol concentration, which caused algal toxicity. Based on the results of the preliminary experiments, a 2-fold dilution was selected as the optimal dilution ratio for this study.

### 2.2. Experimental setup and operation

**2.2.1. Microalgae culture.** For each experiment, 100 μL actively growing microalgal cultured (OD$_{680}$ ≈ 0.8) were maintained in 50 mL Erlenmeyer flask containing 20 mL of WC medium. The inoculum volume was 10% (v/v) of the total culture volume. For the co-culture experiment, the two bacteria (*C. Reinhardtii* and *S. dimorphus*) were co-cultured in 2-fold diluted distillation wastewater (DWW) and prepared by mixing autoclaved raw DWW with deionized water at a ratio of 1 : 1. Cultivation conditions included static growth under 2000 lux illumination (12L:12D cycle) at 20 ± 1 °C, with manual shaking (15 seconds, 3 times daily).

**2.2.2. Culture of microalgae under different nitrogen and phosphorus concentrations.** Nutrient ratio adjustments were performed based on the modified WC medium's baseline formulation, which had a N : P ratio of 4 : 1 by weight. The experimental period lasted for 17 days, during which six different nitrogen-to-phosphorus concentration gradients were tested for *C. reinhardtii*, *S. dimorphus*, and their co-cultivation. The different N : P ratios were achieved by adjusting the concentration of $NaNO_3$ and $K_2HPO_4 \cdot 3H_2O$. The experimental groups had N/P concentrations of 11.6/2.9, 46/11.5, 69/17.25, 103.5/25.9, 155.6/38.9, and 600/150 mg $L^{-1}$, respectively. All cultures were performed in triplicate. Two different sizes of Erlenmeyer flasks were used. 150 mL Erlenmeyer flasks were used with 50 μL of inoculum and 50 mL of growth medium, and 250 mL Erlenmeyer flasks were used with 50 μL of inoculum and 130 mL of growth medium. The 150 mL flasks were used for all tests except for the cultures used for the nutrient analysis, which were grown in the larger 250 mL flasks to allow for a larger volume to be available for analysis. The cultivation conditions were the same as in Section 2.2.1, with a light intensity of 2000 lx at the surface of the culture medium, a temperature of 25 ± 2 °C, and a light cycle of 12 L:12 D, and static cultivation. The position of the Erlenmeyer flasks was rotated daily, and the cultures were manually shaken for 15 seconds, 3 times daily until the microalgae were uniformly suspended in the medium.

To ensure the supply of nutrients, 10 mL of original culture medium was added to the 150 mL Erlenmeyer flask samples every other day to compensate for the algae cell liquid taken for analysis.

**2.2.3. Microalgae culture at different $CO_2$ concentrations.** Industrial-grade $CO_2$ (purity ≥ 99.5%, Chengdu Guangming Gas Co., China) was mixed with compressed air using a gas mixing system (GMS-300 model, accuracy ±2%). Six $CO_2$ concentrations (380, 1000, 3000, 6000, and 9000 ppm) were generated by adjusting the mass flow controllers (MFC) for air and $CO_2$. The pH level was monitored in real-time using a pH sensor (Hach HQ40d). During cultivation, pH, temperature, and light intensity were maintained as described in Section 2.1.

## 2.3. Analytical method

**2.3.1. Growth analysis.** There is a positive correlation between the optical density (OD) of the algal suspension and the biomass of microalgae.[26] The microalgae biomass was represented by the optical density at 680 nm ($OD_{680}$).[27] For growth curve analysis, a 1 mL sample of culture was taken from the 100 mL cultures grown in Section 2.1, and the microalgae were centrifuged at 5000 rpm for 10 minutes. The dry cell weight (DCW) of the microalgae was then determined by drying a known amount of microalgae in a drying oven at 105 °C to a constant weight.[28]

The dry cell weight (DCW) of the microalgae biomass was estimated every other day over 17 days to study the growth curve. The specific growth rate ($\mu$, number of divisions per day) was calculated using the following formula:[29]

$$\mu_m = \frac{\ln X_2 - \ln X_1}{t_2 - t_1} \quad (1)$$

where $\mu$ represents the specific growth rate (d$^{-1}$); $X_2$ and $X_1$ are the biomass concentrations during the exponential phase, and $t_2 - t_1$ represents the time period (d).

**2.3.2. Protein yield determination.** Protein content in the microalgae cells was determined using the Lowry method.[30]

**2.3.3. Determination of nutrient concentration.** To characterize the changes in water quality during microalgae cultivation, a 10 mL sample of the microalgae culture was filtered using a 0.45 μm pore-sized cellulose acetate membrane filter, and the filtrate was used to determine the total phosphorus (TP), total nitrogen (TN), and total chemical oxygen demand (COD). TN and TP were determined using alkaline potassium persulfate digestion UV spectrophotometry (HJ 636-2012), the Nessler reagent method. COD was determined using acidic potassium permanganate titration, respectively. The nutrient absorption rate was calculated using eqn (2) based on the measured TN, TP, and COD content in the 250 mL experimental group. The volume of culture medium removed for measurements was 10 mL.

$$V = \frac{(S_{t-1} - S_t) \times V_{t-1}}{t \times B} \quad (2)$$

where $V$ represents the absorption rate (mg cell$^{-1}$ d$^{-1}$), $S_{t-1}$ and $S_t$ are the nutrient concentrations in the culture medium at time $t-1$ (d) and $t$ (d) (mg L$^{-1}$), $V_{t-1}$ is the volume of the nutrient medium at time $t-1$ (d) (L), $t$ is the time interval between $t-1$ and $t$ (days), and $B$ is the microalgae dry weight (mg).

The nutrient removal rate was calculated using eqn (3) based on the measured nutrient content.

$$r = \frac{C_0 - C_t}{C_0} \times 100\% \quad (3)$$

where $r$ represents the removal rate of TN, TP, and COD (%), $C_0$ is the initial concentration (mg L$^{-1}$), and $C_t$ is the final concentration (mg L$^{-1}$) after cultivation for $t$ (d), respectively.

**2.3.4. Determination of nutrient concentration.** Based on the impact of different N/P concentrations on microalgae growth, three representative concentration gradients were selected: low nutrient group (11.6/2.9 mg L$^{-1}$), optimal nutrient group (46/11.5 mg L$^{-1}$), and high nutrient group (600/150 mg L$^{-1}$). The microalgae were cultivated in the above-mentioned N/P concentration media until the stationary phase (17 days), and the ultrastructural changes of the microalgae were observed using transmission electron microscopy (TEM).

**2.3.5. $CO_2$ fixed rate calculation.** The $CO_2$ fixation rate ($P_{CO_2}$, mg L$^{-1}$ d$^{-1}$) was calculated based on biomass productivity ($P$, mg L$^{-1}$ d$^{-1}$) and carbon content ($C_{carbon}$, %) of *C. reinhardtii* using the following formula:

$$P = \frac{X_2 - X_1}{t_2 - t_1} \quad (4)$$

$$P_{CO_2} = C_{carbon} P \times \frac{M_{CO_2}}{M_C} \quad (5)$$

where $P$ (mg L$^{-1}$ d$^{-1}$) is microalgal biomass productivity, $X_2$ and $X_1$ are the biomass concentrations during the exponential phase, and $t_2 - t_1$ represents the time period (d), $M_{CO_2} = 44$ g

mol$^{-1}$ (molecular weight of CO$_2$), $M_C$ = 12 g mol$^{-1}$ (atomic weight of carbon), $C_{carbon}$ is average carbon content per gram dry cell weight according to measurement using elemental analysis.[31]

## 3. Results and discussion

### 3.1. The growth characteristics of microalgae in distillery wastewater

Growth rate is a very important factor to be determined for microalgal species, which determines the amount of biomass available and the amount of carbon fixed.[32]. The growth trends and specific growth rates of microalgae are shown in Fig. 1a–c, with the specific growth rates shown in Fig. 1d. The different N/P conditions resulted in different growth trends for all cultures. *C. reinhardtii* (Fig. 1a) showed a rapid increase in biomass, entering the exponential growth phase around days 7 to 9 and reaching a maximum of 730 mg L$^{-1}$ at day 9 in the 46/11.5 condition, while *S. dimorphus* (Fig. 1b) and the co-culture (Fig. 1c) showed slower growth. These results indicate that a diluted DWW with a N/P ratio of 4 : 1 can support microalgae cultivation. Although the optimal N/P ratio for microalgal biomass production is generally considered to be 16 : 1,[33,34] the optimal ratio for microalgae still having good growth performance was found to be different in this experiment by 2-fold dilution and maintaining a DWW environment with N/P of approximately 4 : 1. When the initial nitrogen content in the medium exceeds that of phosphorus, microalgae growth primarily depends on nitrogen, which is required for protein synthesis. In the 46/11.5 group, by day 9, when the biomass reached its maximum, the total phosphorus in the medium had decreased sharply, suggesting a reduction in the availability of phosphorus. This could lead to phosphorus starvation, and reduced photosynthetic efficiency,[20] explaining the decline in growth after day 9.

As total nitrogen and other nutrients in the culture medium were consumed, microalgae growth in all groups rapidly entered a decline phase. In the 600/150 (N : P) concentration group, *S. dimorphus* (Fig. 1b) showed a significant reduction in maximum biomass, reaching a value of 250 mg L$^{-1}$, compared to other treatment groups which reached over 500 mg L$^{-1}$. This indicates that high nitrogen and phosphorus concentrations significantly inhibited the growth of *S. dimorphus*. Compared to monoculture conditions, the growth curves under co-culture conditions were more irregular, and the biomass was lower, particularly at later time points, suggesting a competitive relationship between the two microalgae species under these conditions. This suggests that under high nutrient conditions, interspecies competition may play a larger role than under low nutrient conditions.

Although the biomass in the 600/150 concentration group was higher than in the 11.6/2.9 low-phosphorus treatment group, it was still lower than in the other treatment groups, and resulted in a lower overall maximum biomass compared to other groups. This is because phosphorus is considered a limiting factor for growth under low phosphorus conditions; the limited phosphate availability not only reduces the efficiency of the Calvin cycle and carbon fixation capacity, but also restricts the uptake of phosphate, thereby affecting their growth and metabolic activities.[35] In contrast, when phosphorus is not limiting, the phosphate uptake is not restricted.

The specific growth rates of all cultures are shown in Fig. 1d. In general, the specific growth rate of microalgae initially increased and then decreased over time, with all cultures showing a similar maximum specific growth rate (of approximately 0.28 d$^{-1}$), but cultures grown under lower N and P concentrations showing reduced maximum specific growth rates. When the TN/TP ratio was 11.6/2.9, the specific growth rates of *C. reinhardtii*, *S. dimorphus*, and the co-cultivation group were at their lowest (0.186, 0.174, and 0.168 d$^{-1}$, respectively), suggesting that in this condition, both N and P may be limiting for growth, although the low P concentration may be playing a larger role. When the N/P concentrations was 69/17.25, the specific growth rates of *S. dimorphus* and the co-cultivation group began to decrease from day 8 onwards. This may be due to the initial rapid growth and phosphorus uptake, which led to a severe imbalance in the N/P concentrations and the depletion of phosphorus more quickly. Additionally, as the initial nutrient concentration increased, the co-culture became more susceptible to the effects of total phosphorus (TP), possibly due to interspecies competition for the available phosphorus.

### 3.2. Protein synthesis characteristics of diluted distillery wastewater from microalgae culture

The protein content of *C. reinhardtii* and *S. dimorphus*, expressed as a percentage of dry biomass (% DW), showed significant variations under different nitrogen-to-phosphorus (N/P) ratios in diluted brewery wastewater (DWW). For *C. reinhardtii*, protein content peaked on day 15 (7.6% DW) at an N/P ratio of 46/11.5 mg L$^{-1}$ (Fig. 2a). Under low N/P conditions (11.6/2.9 mg L$^{-1}$), the maximum protein content was only 3.5%
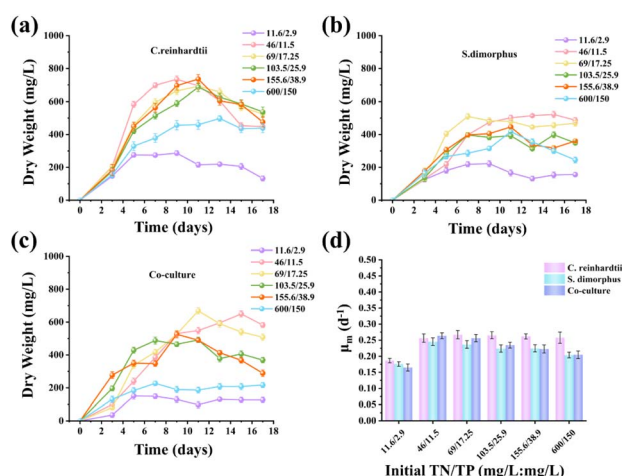


**Fig. 1** Growth characteristics and nutrient removal performance of *C. reinhardtii*, *S. dimorphus*, and their co-culture under different N/P concentrations. (a) Biomass accumulation of *C. reinhardtii*; (b) biomass accumulation of *S. dimorphus*; (c) biomass accumulation of co-culture; (d) specific growth rates. All values are presented as means ± standard deviation (*n* = 3).
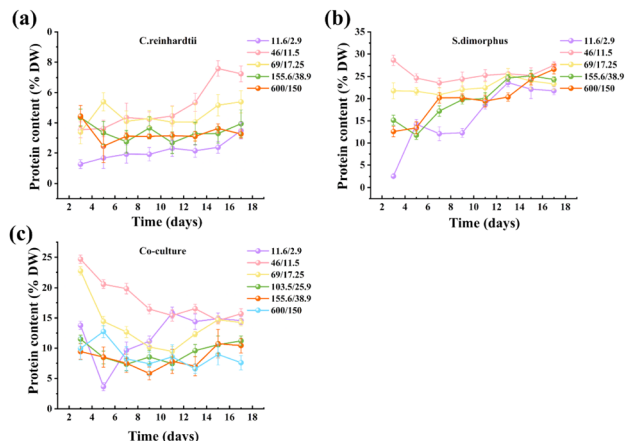
Fig. 2 Changes in protein content over time for *C. reinhardtii*, *S. dimorphus*, and their co-culture under different nitrogen-to-phosphorus (N/P) concentrations in diluted distillery wastewater. (a) Protein content (mg L$^{-1}$) of *C. reinhardtii* over time. (b) Protein content (mg L$^{-1}$) of *S. dimorphus* over time. (c) Protein content (mg L$^{-1}$) of the co-culture over time. All values are presented as means ± standard deviation ($n = 3$).
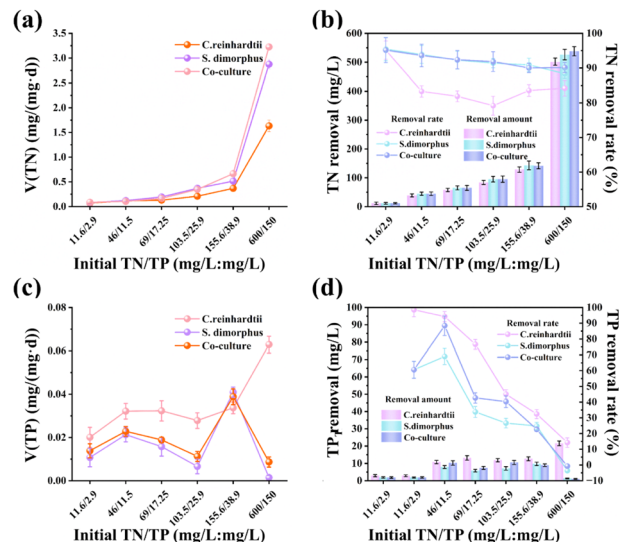


Fig. 3 Nutrient removal performance of *C. reinhardtii*, *S. dimorphus*, and their co-culture under different initial nitrogen-to-phosphorus (N/P) concentrations in diluted distillery wastewater. (a) Total nitrogen (TN) absorption rate (V, mg mg$^{-1}$ d$^{-1}$). (b) TN removal amount (mg L$^{-1}$) and removal rate (%). (c) Total phosphorus (TP) absorption rate (V, mg mg$^{-1}$ d$^{-1}$). (d) TP removal amount (mg L$^{-1}$) and removal rate (%). All values are presented as means ± standard deviation ($n = 3$).

DW, likely due to phosphorus limitation inhibiting ATP-dependent ribosomal activity. This conclusion was supported by TEM observations of mitochondrial vacuolization and membrane rupture (Fig. 5a).[36,37] At high N/P ratios (600/150 mg L$^{-1}$), protein synthesis decreased further to 3.6% DW, potentially caused by cell swelling (Fig. 7) and enzyme activity inhibition in acidified environments from excess $CO_2$.

*S. dimorphus* demonstrated superior protein accumulation capacity, reaching 27.6% DW at the optimal N/P ratio of 46/11.5 mg L$^{-1}$ (Fig. 2b). This performance correlated with its high total nitrogen removal efficiency (95.43%, Fig. 3b). The species preferentially allocated nitrogen to protein synthesis over lipid storage, a metabolic preference aligning with its ecological role in eutrophic wastewater remediation.[38] Intact chloroplasts and well-organized thylakoid layers under optimal N/P conditions (Fig. 6b) enhanced photosynthetic carbon fixation, directly supporting amino acid biosynthesis.[39] However, protein content at the N/P concentration ratio of 600/150 mg L$^{-1}$ was lower than that at 46/11.5 mg L$^{-1}$, reflecting that at high nitrogen concentration, overnutrition led to metabolic disorders, cell division was blocked, and biomass and protein content were lower.[40]

In co-culture systems, the maximum protein content (25.6% DW at 46/11.5 mg L$^{-1}$) was intermediate between those of the two monocultures (Fig. 2c), suggesting phosphorus competition between species. While *S. dimorphus* dominated phosphorus uptake (showing comparable total phosphorus removal to its monoculture, Fig. 3d), *C. reinhardtii* likely experienced protein synthesis inhibition due to phosphorus limitation. In addition, the significant decline in protein content during co-culture may result from competition between carbon (C) and sulfur (S) for ATP-dependent assimilation pathways. For example, sulfur is essential for cysteine and methionine synthesis, which are critical for protein formation. Under nutrient-limited conditions, microalgae prioritize sulfur allocation to antioxidant systems (*e.g.*, glutathione) over protein synthesis, as observed in *Chlamydomonas* by Aburai *et al.*[41] The N/P ratio of 46/11.5 mg L$^{-1}$ optimized nutrient supply and metabolic requirements, promoting efficient protein synthesis while maintaining organelle integrity.[42] This ratio provided sufficient phosphorus for ATP and NADPH production during nitrogen assimilation without causing nutrient inhibition.[43]

### 3.3. Nutrient removal performance of cultured microalgae in diluted distillery wastewater

**3.3.1. Remove nitrogen and phosphorus from wastewater.** The removal efficiency of total nitrogen (TN) by microalgae at different initial N/P concentrations is shown in Fig. 3a and b. When the N/P concentration is 11.6/2.9 mg L$^{-1}$, TN removal efficiency is low (Fig. 3a). This low efficiency is partly due to the nitrogen metabolism of microalgae, which typically relies on the coordinated supply of various nutrient elements. For instance, the abundance of carbon sources and trace elements influences protein synthesis and energy metabolism.[44,45] When carbon and phosphorus are limited in the environment, cells tend to prioritize basic growth needs by regulating metabolic pathways, which may indirectly inhibit nitrogen uptake and assimilation.[46] Additionally, microalgae adjust their intracellular enzyme activity, membrane transporter expression, and metabolic flow distribution in response to external stressors, including nutrient imbalance or excessive/insufficient total nutrient availability, thereby affecting key pathways such as nitrogen uptake and amino acid synthesis.[47] As nitrogen and phosphorus concentrations increase, the TN absorption rates of

both individual algae species and co-culture systems gradually rise (Fig. 3a). This trend is particularly evident at higher N/P concentrations (46/11.5 mg $L^{-1}$ and above), where the absorption rate of the co-culture group is generally higher than that of the individual algae species. Under different N/P concentrations, the three microalgal groups did not show significant differences in TN removal efficiency ($P > 0.05$), although microalgae cultivated under low N/P concentrations showed higher TN removal at the lower concentrations (Fig. 3b), with the 46/11.5 group also showing high removal rates. In the 46/11.5 group, the TN removal efficiency of *S. dimorphus* reached 97.29% on day 17, meeting the TN standard for class IV surface water quality (GB3838-2002), suggesting that this species, under these conditions, could be effectively used for wastewater remediation. According to eqn (3), when the absorption rate of TN by microalgae is constant, a lower microalgal dry weight, would lead to a higher TN absorption rate per mg of algae. In the high-nutrient environment (600/150 group), excessive TN absorption by microalgae (Fig. 3a) was detrimental to algal growth, which ultimately led to a decline in TN removal efficiency (Fig. 3b).

Phosphorus is a fundamental macronutrient for microalgae, and potassium hydrogen phosphate ($K_2HPO_4$) can be directly transported into microalgal cells through membrane transport proteins, where it participates in the synthesis of nucleic acids, adenosine triphosphate (ATP), and membrane phospholipids,[48] and may be removed from the system through phosphate precipitation. The changes in TP absorption rates in the culture media of each experimental group are shown in Fig. 3c, while the final TP removal rates and removal efficiencies are presented in Fig. 3d. As mentioned in ref. 49, previous studies have indicated that phosphorus absorption decreases under low nitrogen conditions. This study found that under the lowest N/P concentration (11.6/2.9 mg $L^{-1}$), *C. reinhardtii* showed a very high phosphorus absorption rate (Fig. 3c), and a final TP removal efficiency of close to 100% after 17 days (Fig. 3d). In the 46/11.5 group, *S. dimorphus* removed 7.84 mg $L^{-1}$ of TP, with a final removal efficiency of 68.94% after 17 days. This may be because when the culture medium contains an appropriate level of phosphorus, phosphorus-starved algal cells may accumulate more phosphorus, possibly through a hunger-driven absorption mechanism.[50]

When the N/P concentration increased to 600/150 mg $L^{-1}$, the high nutrient environment caused significant stress to *S. dimorphus*, leading to a reduced biomass, which led to a release of phosphates, and an increase in TP concentration (Fig. 3d).[51] The TP removal efficiency decreased with increasing initial N and P concentration. Throughout the experimental period, *C. reinhardtii* exhibited a higher TP removal efficiency at most initial concentrations than *S. dimorphus*, particularly at lower nutrient concentrations (Fig. 3d), with *C. reinhardtii* showing much higher TP removal at the lowest N and P concentrations. Under co-culture conditions, the TP removal effect was consistent with that of *S. dimorphus*, suggesting that *S. dimorphus* plays a dominant role in wastewater nutrient utilization and may inhibit *C. reinhardtii*'s ability to absorb TP.

**3.3.2. Remove COD from wastewater.** All culture media showed a reduction in organic compounds, represented by changes in COD during the cultivation process, as shown in Fig. 4a–c. The trends in COD reduction (Fig. 4a–c) largely mirrored the growth trends of the microalgal cultures (Fig. 1a–c). As the microalgae grew, COD decreased significantly ($p < 0.05$, using ANOVA with Tukey *post hoc* analysis), particularly during the exponential growth phase. Co-culture provided a higher COD removal rate compared to monoculture groups at most conditions, which is consistent with the findings of Hu *et al.*,[52] who suggested that the high COD utilization efficiency can be attributed to competition between different microalgal species, which may also enhance organic matter reduction. However, after day 13, COD levels gradually increased in some of the groups, (particularly at lower N and P conditions), which may be due to both a reduction in nutrients and insufficient light, which may have caused the algae to secrete more organic matter. Therefore, in the high-nutrient environment (600/150 group), the COD consumption was not as large, with this group showing a higher final COD at the end of the experiment compared to the other groups, although COD removal was rapid at early time points. This suggests that the high nutrient groups had less organic material for the microalgae and other heterotrophic microorganisms to break down.

In the distillery wastewater with an initial N/P concentrations of 4 : 1, *S. dimorphus* and the co-culture group showed a higher COD removal efficiency than *C. reinhardtii*. The final COD values at this N/P concentrations were 260 mg $L^{-1}$ for *C. reinhardtii*, and 160 and 140 mg $L^{-1}$ for *S. dimorphus* and the co-culture, respectively, as shown in Fig. 4d. However, at high initial N/P concentrations (600/150 group), the final COD removal ability of *C. reinhardtii* was more stable, and *C. reinhardtii* and the co-culture group showed a higher final COD removal, compared to *S. dimorphus*, as shown in Fig. 4d. This
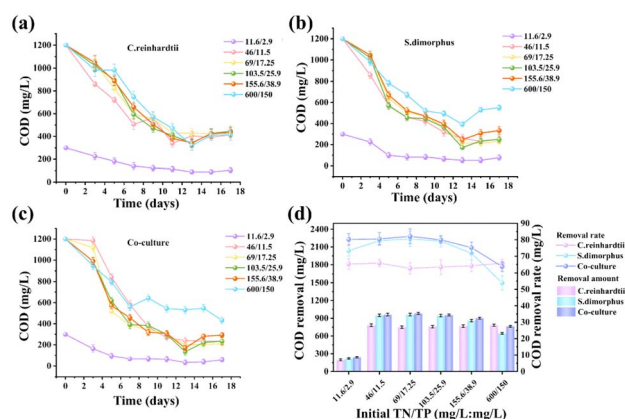


**Fig. 4** Chemical Oxygen Demand (COD) removal performance of *C. reinhardtii*, *S. dimorphus*, and their co-culture under different initial nitrogen-to-phosphorus (N/P) concentrations in diluted distillery wastewater. (a) COD content (mg $L^{-1}$) of *C. reinhardtii* over time. (b) COD content (mg $L^{-1}$) of *S. dimorphus* over time. (c) COD content (mg $L^{-1}$) of the co-culture over time. (d) COD removal amount (mg $L^{-1}$) and removal rate (%) at day 17. All values are presented as means ± standard deviation ($n = 3$).

indicates that *C. reinhardtii* has a higher COD removal ability at high-N/P and low-N/P concentrations, suggesting that it may be more suitable for treating undiluted distillery wastewater.

### 3.4. Ultrastructural changes of distillery wastewater after microalgae culture

Fig. 5 shows the ultrastructure of *C. reinhardtii* (a) and *S. dimorphus* (b) when cultured under the low N/P conditions (11.6/2.9 mg L$^{-1}$). Under these low N/P conditions, mitochondrial cavitation and membrane rupture were observed in *C. reinhardtii* cells (Fig. 5a), which can impair oxygen respiration and disrupt energy conversion, potentially contributing to the reduced growth observed under these conditions. This may be attributed to excessive phosphorus leading to the over-accumulation of polyphosphate within the cells, which disrupts membrane permeability and enzyme function.[53] Compared to *C. reinhardtii*, the effects of low nutrient concentrations on the organelles of *S. dimorphus* were more pronounced (Fig. 5b): the chloroplast structure appeared significantly deformed, and the thylakoid lamellae were disorganized or even indistinct, severely impairing photosynthesis. The cell wall exhibited severe wrinkling, with partial degradation, and some organelles appeared to be disintegrated or dissolved, resulting in cavitation. Under nitrogen and phosphorus deficiency, both the photosynthetic function of the chloroplast and the respiratory function of the mitochondria were damaged, reducing the performance of this culture as compared to *C. reinhardtii* as seen in Fig. 1 and 2.
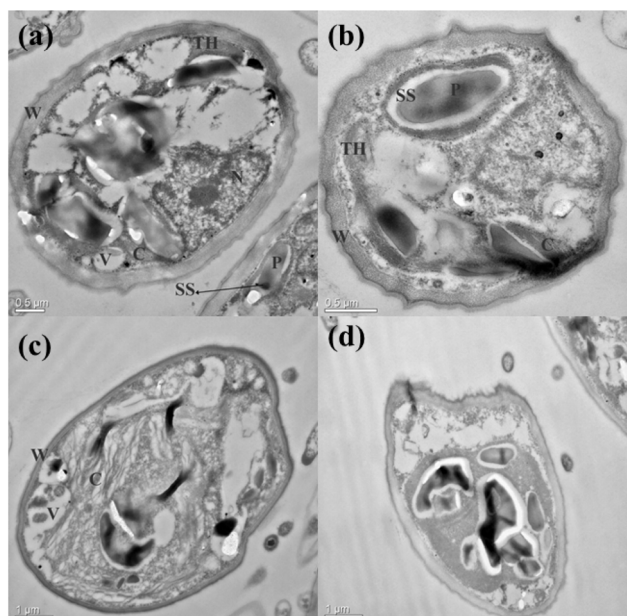
Fig. 6 shows the ultrastructure of *C. reinhardtii* (a) and *S. dimorphus* (b) when cultured under optimal N/P conditions (46/11.5 mg L$^{-1}$). Under these optimal N/P concentrations, *C. reinhardtii* exhibited the best growth and resource utilization of nitrogen and phosphorus among the experimental groups, as shown in Fig. 1 and 2. Under this condition, the chloroplasts appeared to be larger, and the pyrenoid within the chloroplasts increased in size, surrounded by a starch sheath, suggesting that the cells were actively fixing carbon and storing the results of that carbon fixation. The thylakoid layers were distinct and well-organized. Mitochondria also appeared to be larger, with intact structures, including inner and outer membranes (Fig. 6a). These findings suggest that these nutrient conditions can enhance cellular photosynthesis and respiration, as has been observed by the higher growth and protein content of these cultures. In comparison, *S. dimorphus* showed more pronounced impacts of environmental conditions on its cellular ultrastructure (Fig. 6b). Although its growth and nutrient utilization of nitrogen and phosphorus were also optimal under this condition, its overall performance was inferior to that of *C. reinhardtii*. The thylakoid layers in *S. dimorphus* were less dense and looser compared to those in *C. reinhardtii*, indicating a lower photosynthetic capacity. These observations are consistent with the functional data, and shows that the growth characteristics of *S. dimorphus* under these conditions are consistent with its cellular structure and remain less favorable than those of *C. reinhardtii*.

Fig. 7 shows the ultrastructure of *C. reinhardtii* (a) and *S. dimorphus* (b) when cultured under high N/P conditions (600/150 mg L$^{-1}$). Under these high-nutrient conditions, the cells of both *C. reinhardtii* and *S. dimorphus* were larger than those in the low (Fig. 5) and optimal (Fig. 6) experimental groups, possibly due to excessive nitrogen and phosphorus absorption, leading to cell swelling (Fig. 7a and b). Most organelles in the microalgae cells appeared severely damaged and deformed, with indistinguishable structures, leaving the cells on the verge of death. Vacuoles appeared abnormally abundant, with reduced or dissolved contents. Some chloroplasts shrank or deformed, the thylakoid layer structures became disordered, and severe plasmolysis occurred. These morphological changes indicate that the cultures were under considerable stress, which
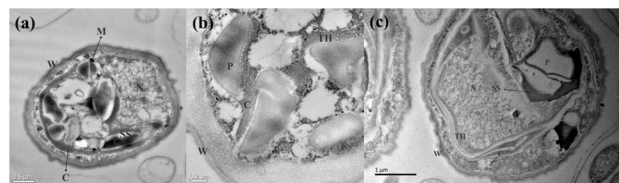


**Fig. 5** Transmission electron microscopy (TEM) images showing the ultrastructure of *C. reinhardtii* (a and b) and *S. dimorphus* (c and d) cells grown under low nitrogen-to-phosphorus (N/P) conditions (11.6/2.9 mg L$^{-1}$). Key cellular components are labeled: C – chloroplast, N – nucleus (nucleolus), P – protein nucleus, SS – starch sheath, V – vacuole, TH – thylakoid, W – cell wall. Scale bars indicate 0.5 μm in (a and b) and 1 μm in (c and d).



**Fig. 6** Transmission electron microscopy (TEM) images showing the ultrastructure of *C. reinhardtii* (a and b) and *S. dimorphus* (c) cells grown under optimal nitrogen-to-phosphorus (N/P) conditions (46/11.5 mg L$^{-1}$). Key cellular components are labeled: C – chloroplast, N – nucleus (nucleolus), P – protein nucleus, SS – starch sheath, V – vacuole, TH – thylakoid, W – cell wall. Scale bars indicate 0.5 μm in (a and b) and 1 μm in (c).
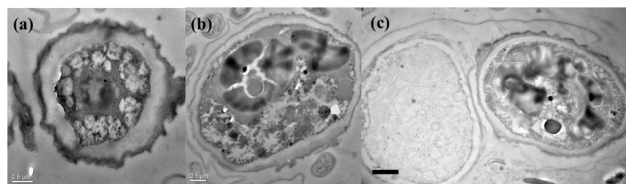
**Fig. 7** Transmission electron microscopy (TEM) images showing the ultrastructure of *C. reinhardtii* (a and b) and *S. dimorphus* (c) cells grown under optimal nitrogen-to-phosphorus (N/P) conditions (46/11.5 mg L$^{-1}$). Key cellular components are labeled: C – chloroplast, N – nucleus (nucleolus), P – protein nucleus, SS – starch sheath, V – vacuole, TH – thylakoid, W – cell wall. Scale bars indicate 0.5 μm in (a) and (b) and 1 μm in (c).



**Fig. 8** Growth and physiological responses of *C. reinhardtii* under different $CO_2$ concentrations. (a) Growth curve showing the dry weight (mg L$^{-1}$) of *C. reinhardtii* over time. (b) Specific growth rate ($\mu$, d$^{-1}$) and culture medium pH at different $CO_2$ concentrations. All values are presented as means ± standard deviation ($n = 3$).

has likely contributed to their reduced growth and nutrient uptake performance.

# 4. Biological carbon sequestration mechanism of *C. reinhardtii* cultivated by DWW

From the observations in the previous experimental stages, the dry weight of *C. reinhardtii* was consistently higher than that of *S. dimorphus* under the low and optimal conditions, as shown in Fig. 1a and b, with similar performance at high N/P concentrations. Therefore, in this stage, the study simulates the $CO_2$ concentration in flue gas emissions from power plants, based on the atmospheric $CO_2$ concentration in natural environments, to explore the use of different $CO_2$ concentrations as an external carbon source for cultivating *C. reinhardtii*. This preliminary investigation into the carbon sequestration capacity of *C. reinhardtii* lays the groundwork for utilizing distillery wastewater to cultivate bioenergy microalgae and achieve efficient carbon fixation.

## 4.1. Effects of different $CO_2$ concentrations on the growth of *Chlamydomonas reinhardtii*

$CO_2$ concentration directly affects the photosynthetic efficiency and growth of microalgae. While microalgae can tolerate a certain range of $CO_2$ concentrations, concentrations beyond this range significantly inhibit growth and carbon sequestration capacity. Therefore, determining the optimal $CO_2$ concentration is critical for achieving maximum biomass and protein yields for specific microalgae species,[54] and is important for practical industrial applications. In this experimental phase, the initial inoculum concentration was relatively low (4.22 mg L$^{-1}$) to ensure a clear analysis of growth rates, since high initial concentrations can affect the overall growth curve. The results showed that under atmospheric $CO_2$ levels (380 ppm), *C. reinhardtii* rapidly entered the exponential growth phase, with biomass reaching 704 mg L$^{-1}$ on day 11 and a specific growth rate of 0.465 d$^{-1}$, as shown in Fig. 8a. At 3000 ppm $CO_2$, *C. reinhardtii* exhibited slower growth during the first three days but then quickly transitioned into the exponential growth phase, achieving a biomass of 825 mg L$^{-1}$ on day 13 with a specific growth rate of 0.406 d$^{-1}$, as shown in Fig. 8a. This
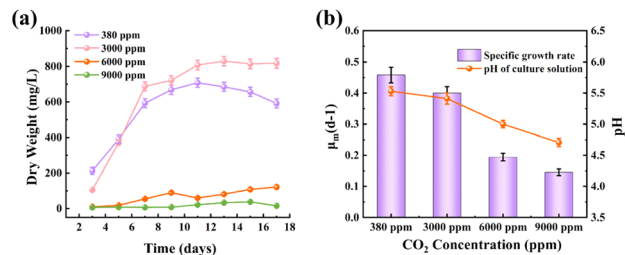
indicates that 3000 ppm $CO_2$ enhances biomass accumulation. However, under 6000 ppm and 9000 ppm $CO_2$ conditions, *C. reinhardtii* experienced a 1–7 days adaptation period, which was characterised by a slow growth, followed by even slower growth. Notably, biomass accumulation was negligible in the 9000 ppm group, as shown in Fig. 8a.

Wang *et al.*[55] found that decreasing $CO_2$ concentrations within the range of 50% to 6% caused changes in tryptophan metabolites due to $CO_2$ deficiency, resulting in division inhibition and growth stagnation, with high $CO_2$ levels showing negative effects on growth, consistent with what has been found in the current study at high $CO_2$ levels.

At low $CO_2$ concentrations, the solubility of $CO_2$ in water and the affinity of Rubisco for $CO_2$ are relatively low.[56] While higher $CO_2$ concentrations provide more carbon sources, they simultaneously increase carbonic acid formation, leading to a decrease in pH, as shown in Fig. 8b, where the pH dropped from 5.54 to 4.72 as $CO_2$ concentrations increased from 380 ppm to 9000 ppm. While the pH of the microalgal culture medium plays a role in regulating nutrient absorption, photosynthetic activity, and carbon fixation efficiency,[57] the optimal pH range is difficult to maintain when using $CO_2$ as an external carbon source, due to increased carbonic acid formation which results in a decrease in pH. Optimal or slightly alkaline conditions promote the conversion of $CO_2$ to $HCO_3^-$, allowing microalgae to concentrate $HCO_3^-$ within their cells *via* bicarbonate pumps. This process, facilitated by carbonic anhydrase or the Calvin cycle, enhances $CO_2$ capture and promotes microalgal growth.[58,59] However, under acidic conditions, chloroplast stroma acidification impairs the conversion of $HCO_3^-$ to $CO_2$, inactivating key enzymes of the Calvin cycle. This ultimately inhibits microalgal growth and reduces carbon assimilation efficiency.[60,61]

## 4.2. Effects of different $CO_2$ concentrations on protein content of *Chlamydomonas reinhardtii*

As shown in Fig. 9, the protein content trends in the 380 ppm and 3000 ppm groups were similar, with both increasing with cultivation time, and reaching a maximum around day 13, followed by a slow decline. At a $CO_2$ concentration of 3000 ppm, *C. reinhardtii* exhibited the maximum protein content, peaking at
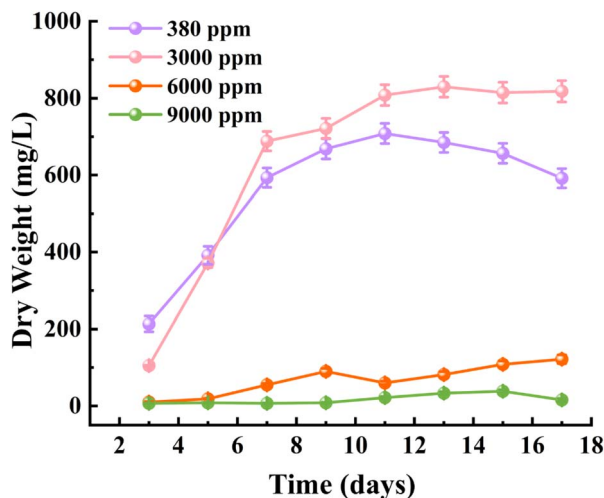
**Fig. 9** Changes in protein content of *C. reinhardtii* over time under different $CO_2$ concentrations. Protein content is presented as mg $L^{-1}$. All values are presented as means ± standard deviation ($n = 3$).

45.28 mg $L^{-1}$ on day 13, consistent with the maximum dry weight achieved in this group, as shown in Fig. 8a. This might be attributed to the availability of an appropriate carbon source, which promoted *C. reinhardtii*'s cellular metabolism and growth, thereby enhancing the synthesis of primary metabolites such as proteins.

In contrast, the 6000 ppm and 9000 ppm groups both showed the lowest protein content, with the 6000 ppm group reaching a value of only 3.54 mg $L^{-1}$ at day 17, and the values for the 9000 ppm group being similarly negligible at all time points, as shown in Fig. 9. Studies have shown that elevated $CO_2$ environments can enhance the transcription and translation of related genes and proteins (*e.g.*, Rubisco), thereby boosting photosynthesis, carbon metabolism, protein synthesis, and lipid accumulation. However, excessively high $CO_2$ concentrations can inhibit microalgal growth.[62,63] This inhibition is primarily due to the increased acidity of the culture medium caused by high $CO_2$ levels, which suppresses the normal physiological activities of *C. reinhardtii*, as linked to the pH changes shown in Fig. 8b. Consequently, the synthesis of intracellular components such as proteins is reduced, and cell division and growth are slowed or obstructed[64] in *C. reinhardtii*.

### 4.3 Carbon sequestration capacity analysis of *C. reinhardtii*

The $CO_2$ fixation rate of *C. reinhardtii* under different $CO_2$ concentrations is shown in Table 3, At 3000 ppm $CO_2$, the $CO_2$ fixation rate of *C. reinhardtii* reached its peak (84.07 mg $L^{-1}$ $d^{-1}$), consistent with the observed peak biomass productivity (50.95 mg $L^{-1}$ $d^{-1}$). This indicates that moderate $CO_2$ enrichment enhances photosynthetic efficiency and carbon assimilation, likely due to sufficient carbon availability for the Calvin cycle.[65] At 6000 and 9000 ppm $CO_2$, the fixation rates dropped sharply to 13.16 and 1.05 mg $L^{-1}$ $d^{-1}$, respectively. This decline correlates with the pH reduction (from 5.54 to 4.72, Fig. 8b), which disrupts cellular pH homeostasis and inhibits Rubisco

enzyme activity.[66] Additionally, excessive $CO_2$ may induce oxidative stress, further impairing metabolic functions.[67] The fixation rate at 3000 ppm (84.07 mg $L^{-1}$ $d^{-1}$) aligns with studies on *Chlorella vulgaris* (50–150 mg $L^{-1}$ $d^{-1}$), validating the feasibility of using *C. reinhardtii* for carbon capture in DWW. However, at 9000 ppm, *C. reinhardtii* is severely inhibited, in contrast to some extremophilia such as *Scenedesmus* sp., which can tolerate up to 100% $CO_2$,[68] highlighting species-specific adaptability. The results suggest that *C. reinhardtii* can be integrated into industrial flue gas treatment systems (typically 10–25% $CO_2$)[69] after dilution to 3000 ppm. This approach not only reduces $CO_2$ emissions but also generates biomass for bioenergy production, achieving dual environmental and economic benefits.

## 5. Conclusions

This study demonstrates that coupling distillery wastewater (DWW) treatment with microalgae cultivation for $CO_2$ fixation offers a promising approach for simultaneous bioremediation, biomass production, and carbon capture. Specifically, an N/P concentration of 46/11.5 mg $L^{-1}$ enabled efficient nutrient removal and resulted in high biomass and protein accumulation for both *C. reinhardtii* and *S. dimorphus*. However, excessive or insufficient nutrients significantly inhibited microalgal growth and performance, leading to reduced nutrient uptake, and resulted in structural changes such as cell wall separation, abnormal vacuole proliferation, and chloroplast contraction, as was shown in the experimental data.

Although the carbon sequestration results obtained in this study with microalgae are preliminary, the observed increase in biomass at specific $CO_2$ concentrations, particularly at 3000 ppm, indicates a potential for future carbon capture strategies using microalgae and DWW. Future research should explore the optimization of $CO_2$ delivery systems and bioreactor designs to maximize microalgal carbon fixation, as well as address any limitations associated with scale-up, specifically with respect to high-density cultures. In conclusion, this study provides an innovative and economically feasible method for DWW treatment by integrating microalgae cultivation with $CO_2$ fixation, highlighting the potential of microalgae for both resource recovery and environmental protection. Future work should focus on optimizing the N/P ratios and $CO_2$ delivery, testing the process on undiluted DWW, and exploring the economic feasibility of this method for practical applications in wastewater treatment and bioenergy production.

## Data availability

All data supporting this study are included within the article.

## Author contributions

All authors contributed to the study conception and design. The experiment was carried out by Han Yuan, Xinyue Huangpeng, Zhi Huang. Material preparation, data collection and analysis were performed by Han Yuan, Jiang Yu, Siwei Deng, Yinying

Jiang. The first draft of the manuscript was written by Han Yuan. All authors commented on previous versions of the manuscript. All authors read and approved the final manuscript.

## Conflicts of interest

There are no conflicts to declare.

## Acknowledgements

## Notes and references

1 Y. Ravikumar, S. A. Razack, J. Yun and G. Zhang, Recent advances in Microalgae-based distillery wastewater treatment, *Environ. Technol. Innovation*, 2021, **24**, 101839.

2 J. Fito, N. Tefera, H. Kloos and S. W. Van Hulle, Physicochemical Properties of the Sugar Industry and Ethanol Distillery Wastewater and Their Impact on the Environment, *Sugar Tech*, 2019, **21**, 265–277.

3 I. Johnson, C. Krishnan and M. Kumar, Enhancing nutrient bioavailability in distillery wastewater through electrochemical oxidation for microalgal growth: insights on biomass yield, nutrient utilisation, and VFA-assisted carbon capture, *Algal Res.*, 2024, **83**, 103734.

4 H. Santana, *et al.*, Microalgae cultivation in sugarcane vinasse: selection, growth and biochemical characterization, *Bioresour. Technol.*, 2017, **228**, 133–140.

5 S. Krishnamoorthy, P. Manickam and V. Muthukaruppan, Evaluation of distillery wastewater treatability in a customized photobioreactor using blue-green microalgae—laboratory and outdoor study, *J. Environ. Manage.*, 2019, **234**, 412–423.

6 S. Ratna, S. Rastogi and R. Kumar, Current trends for distillery wastewater management and its emerging applications for sustainable environment, *J. Environ. Manage.*, 2021, **290**, 112544.

7 Y. Song, *et al.*, The promising way to treat wastewater by microalgae: approaches, mechanisms, applications and challenges, *J. Water Process Eng.*, 2022, **49**, 103012.

8 J. Wang, Q. Tian, W. Zeng, G. Qiu and L. Shen, Insights about fungus-microalgae symbiotic system in microalgae harvesting and wastewater treatment: a review, *Renewable Sustainable Energy Rev.*, 2023, **182**, 113408.

9 A. Azimi, *et al.*, Removal of Heavy Metals from Industrial Wastewaters: A Review, *ChemBioEng Rev.*, 2017, **4**, 37–59.

10 A. Bhatt, *et al.*, Assessing sustainability of microalgae-based wastewater treatment: environmental considerations and impacts on human health, *J. Environ. Manage.*, 2024, **354**, 120435.

11 W. Dou, X. Peng, L. Kong and X. Hu, A review on the removal of Cl(-I) with high concentration from industrial wastewater: approaches and mechanisms, *Sci. Total Environ.*, 2022, **824**, 153909.

12 Y. Wu, J. Yu and Z. Huang, Migration of total petroleum hydrocarbon and heavy metal contaminants in the soil–groundwater interface of a petrochemical site using machine learning: impacts of convection and diffusion, *RSC Adv.*, 2024, **14**, 32304.

13 J. T. Zhang, *et al.*, Microalgal-bacterial biofilms for wastewater treatment: operations, performances, mechanisms, and uncertainties, *Sci. Total Environ.*, 2024, **907**, 167974.

14 M. Zubair, *et al.*, Biological nutrient removal and recovery from solid and liquid livestock manure: recent advance and perspective, *Bioresour. Technol.*, 2020, **301**, 122823.

15 F. Li, *et al.*, Cultivation of *Chlorella vulgaris* in membrane-treated industrial distillery wastewater: growth and wastewater treatment, *Front. Environ. Sci.*, 2021, **9**, 770633.

16 S. Vasistha, *et al.*, Microalgae on distillery wastewater treatment for improved biodiesel production and cellulose nanofiber synthesis: a sustainable biorefinery approach, *Chemosphere*, 2023, **315**, 137666.

17 A. Devi, *et al.*, Microalgae: a green eco-friendly agents for bioremediation of tannery wastewater with simultaneous production of value-added products, *Chemosphere*, 2023, **336**, 139192.

18 A. Zhang, S. Fang and M. Ge, *et.al.*, Microalgae-derived hydrogels/membranes for phosphorus removal and recovery from aquaculture tailwater: waste utilization and phosphorus recycling, *Bioresour. Technol.*, 2024, **409**, 131246.

19 C. Zhang, S. Li and S. H. Ho, Converting nitrogen and phosphorus wastewater into bioenergy using microalgae-bacteria consortia: a critical review, *Bioresour. Technol.*, 2021, **342**, 126056.

20 X. Y. Liu, *et al.*, Performance and mechanism of *Chlorella* in swine wastewater treatment: roles of nitrogen-phosphorus ratio adjustment and indigenous bacteria, *Bioresour. Technol.*, 2022, **358**, 127402.

21 Q. Wang, *et al.*, Growth enhancement of biodiesel-promising microalga *Chlorella pyrenoidosa* in municipal wastewater by polyphosphate-accumulating organisms, *J. Cleaner Prod.*, 2019, **240**, 118148.

22 R. Wang, X. Wang and T. Zhu, Research progress and application of carbon sequestration in industrial flue gas by microalgae: a review, *J. Environ. Sci.*, 2025, **152**, 14–288.

23 M. Derakhshandeh, T. Atici and U. Tezcan Un, Evaluation of Wild-Type Microalgae Species Biomass as Carbon Dioxide Sink and Renewable Energy Resource, *Waste Biomass Valorization*, 2021, **12**, 105–121.

24 R. Prasad, *et al.*, Role of microalgae in global $CO_2$ sequestration: physiological mechanism, recent development, challenges, and future prospective, *Sustainability*, 2021, **13**(23), 13061.

25 Z. He, *et al.*, Cultivation of *Chlorella pyrenoidosa* and *Scenedesmus obliquus* in swine wastewater: nitrogen and phosphorus removal and microalgal growth, *Process Saf. Environ. Prot.*, 2023, **179**, 887–895.

26 M. Birkholz, *et al.*, Separation of heterotrophic microalgae *Crypthecodinium cohnii* by dielectrophoresis, *Front. Bioeng. Biotechnol.*, 2022, **10**, 855035.

27 M. Bhandari, S. Kharkwal and S. K. Prajapati, Recycling drinking water RO reject for microalgae-mediated resource recovery, *Resour. Conserv. Recycl.*, 2023, **188**, 106699.

28 Z. He, *et al.*, Cultivation of *Scenedesmus obliquus* and *Chlorella pyrenoidosa* in Municipal Wastewater Using Monochromatic and White LED as Light Sources, *Waste Biomass Valorization*, 2021, **12**, 4873–4883.

29 M. Levasseur, P. A. Thompson and P. J. Harrison, Physiological acclimation of marine phytoplankton to different nitrogen sources, *J. Phycol.*, 1993, **29**, 587–595.

30 C. V. G. López, *et al.*, Protein measurements of microalgal and cyanobacterial biomass, *Bioresour. Technol.*, 2010, **101**(19), 7587–7591.

31 M. A. Kassim and T. K. Meng, Carbon dioxide ($CO_2$) biofixation by microalgae and its potential for biorefinery and biofuel production, *Sci. Total Environ.*, 2017, **584–585**, 1121–1129.

32 M. Derakhshandeh, T. Atici and U. Tezcan Un, Evaluation of Wild-Type Microalgae Species Biomass as Carbon Dioxide Sink and Renewable Energy Resource, *Waste Biomass Valorization*, 2020, **12**, 105–121.

33 J. Li, *et al.*, Enhancement of ammonium removal from landfill leachate using microalgae by an integrated strategy of nutrient balance and trophic mode conversion, *Algal Res.*, 2022, **61**, 102572.

34 S. M. Z. Hossain, *et al.*, Soft-computing modeling and multiresponse optimization for nutrient removal process from municipal wastewater using microalgae, *J. Water Process Eng.*, 2022, **45**, 102490.

35 X. Lian, *et al.*, A new microalgal negative carbon technology for landfill leachate treatment: Simultaneous removal of nitrogen and phosphorus, *Sci. Total Environ.*, 2024, **948**, 174779.

36 C. Oz Yasar, L. Fletcher and M. A. Camargo-Valero, Effect of macronutrients (carbon, nitrogen, and phosphorus) on the growth of *Chlamydomonas reinhardtii* and nutrient recovery under different trophic conditions, *Environ. Sci. Pollut. Res.*, 2023, **30**, 111369–111381.

37 M. Kamalanathan, *et al.*, Impacts of nitrogen and phosphorus starvation on the physiology of *Chlamydomonas reinhardtii*, *J. Appl. Phycol.*, 2016, **28**, 1509–1520.

38 K. Jothibasu, *et al.*, Impact of microalgal cell wall biology on downstream processing and nutrient removal for fuels and value-added products, *Biochem. Eng. J.*, 2022, **187**, 108642.

39 M. P. Sinetova, A. G. Markelova and D. A. Los, The effect of nitrogen starvation on the ultrastructure and pigment composition of chloroplasts in the acidothermophilic microalga *Galdieria sulphuraria*, *Russ. J. Plant Physiol.*, 2006, **53**, 153–162.

40 Y. Wang, *et al.*, Response of energy microalgae *Chlamydomonas reinhardtii* to nitrogen and phosphorus stress, *Environ. Sci. Pollut. Res.*, 2018, **25**, 5762–5770.

41 N. Aburai, *et al.*, Mutual supply of carbon and nitrogen sources in the co-culture of aerial microalgae and nitrogen-fixing bacteria, *Algal Res.*, 2023, **70**, 103001.

42 W. Cao, *et al.*, The response to inorganic phosphates forms for mariculture wastewater treatment with microalgae: biochemical component synthesis, cellular morphology and phosphorus storage, *Process Saf. Environ. Prot.*, 2024, **188**, 480–491.

43 K. Kumari, *et al.*, Nitrogen, phosphorus and high $CO_2$ modulate photosynthesis, biomass and lipid production in the green alga *Chlorella vulgaris*, *Photosynth. Res.*, 2021, **148**, 17–32.

44 Y. Su, *et al.*, Revisiting carbon, nitrogen, and phosphorus metabolisms in microalgae for wastewater treatment, *Sci. Total Environ.*, 2021, **762**, 144590.

45 X. Li, *et al.*, Role of nitrogen transport for efficient energy conversion potential in low carbon and high nitrogen/phosphorus wastewater by microalgal-bacterial system, *Bioresour. Technol.*, 2022, **351**, 127019.

46 M. Giordano and L. Prioretti Sulphur and Algae: Metabolism, Ecology and Evolution. *The Physiology of Microalgae*, 2016, pp. 185–209.

47 D. Singh, L. Nedbal and O. Ebenhöh, Modelling phosphorus uptake in microalgae, *Biochem. Soc. Trans.*, 2018, **46**, 483–490.

48 C. Zhang, S. Li and S. H. Ho, Converting nitrogen and phosphorus wastewater into bioenergy using microalgae-bacteria consortia: a critical review, *Bioresour. Technol.*, 2021, **342**, 126056.

49 E. M. Salgado, A. F. Esteves, A. L. Gonçalves and J. Pires, Microalgal cultures for the remediation of wastewaters with different nitrogen to phosphorus ratios: process modelling using artificial neural networks, *Environ. Res.*, 2023, **231**, 116076.

50 J. I. Navarro, *et al.*, Elemental and macromolecular plasticity of *Chlamydomonas reinhardtii* (Chlorophyta) in response to resource limitation and growth rate, *J. Phycol.*, 2024, **60**, 418–431.

51 W. Cao, Y. Xing, D. Xing, Y. Zhao, M. Gao, C. Jin and L. Guo, The response to inorganic phosphates forms for mariculture wastewater treatment with microalgae: biochemical component synthesis, cellular morphology and phosphorus storage, *Process Saf. Environ. Prot.*, 2024, **188**, 480–491.

52 D. Hu, J. Zhang, R. Chu, Z. Yin, J. Hu, Y. K. Nugroho, Z. Li and L. Zhu, Microalgae *Chlorella vulgaris* and *Scenedesmus dimorphus* co-cultivation with landfill leachate for pollutant removal and lipid production, *Bioresour. Technol.*, 2021, **342**, 126003.

53 Q. Wu, L. Guo, X. Li and Y. Wang, Effect of phosphorus concentration and light/dark condition on phosphorus uptake and distribution with microalgae, *Bioresour. Technol.*, 2021, **340**, 125745.

54 R. K. Mohapatra, D. Padhi, R. Sen and M. Nayak, Bio-inspired $CO_2$ capture and utilization by microalgae for bioenergy feedstock production: a greener approach for environmental protection, *Bioresour. Technol. Rep.*, 2022, **19**, 101116.

55 Z. Wang, J. Cheng, Y. Sun, D. Jia, Y. Tang, W. Yang and K. Cen, Comprehensive understanding of regulatory mechanisms, physiological models and key enzymes in microalgal cells based on various concentrations of $CO_2$, *Chem. Eng. J.*, 2023, **454**, 140233.

56 A. Mustafa, B. G. Lougou, Y. Shuai, Z. Wang and H. Tan, Current technology development for $CO_2$ utilization into solar fuels and chemicals: a review, *J. Energy Chem.*, 2020, **49**, 96–123.

57 V. A. Thiviyanathan, P. J. Ker, S. G. Hoon Tang, E. P. P. Amin, W. Yee, M. A. Hannan, Z. Jamaludin, L. D. Nghiem and T. M. I. Mahlia, Microalgae biomass and biomolecule quantification: optical techniques, challenges and prospects, *Renewable Sustainable Energy Rev.*, 2024, **189**, 113926.

58 M. A. Kassim and T. K. Meng, Carbon dioxide ($CO_2$) biofixation by microalgae and its potential for biorefinery and biofuel production, *Sci. Total Environ.*, 2017, **584–585**, 1121–1129.

59 R. K. Goswami, S. Mehariya and P. Verma, Advances in microalgae-based carbon sequestration: current status and future perspectives, *Environ. Res.*, 2024, **249**, 118397.

60 A. Tarafdar, G. Sowmya, K. Yogeshwari, R. Gurdeep, T. Negi, M. K. Awasthi, A. Hoang, R. Sindhu and R. Sirohi, Environmental pollution mitigation through utilization of carbon dioxide by microalgae, *Environ. Pollut.*, 2023, **328**, 121623.

61 J. Zeng, Z. Wang and G. Chen, Biological characteristics of energy conversion in carbon fixation by microalgae, *Renewable Sustainable Energy Rev.*, 2021, **152**, 111661.

62 Y. Chen, C. Xu and S. Vaidyanathan, Influence of gas management on biochemical conversion of $CO_2$ by microalgae for biofuel production, *Appl. Energy*, 2020, **261**, 114420.

63 K. Li, J. Cheng, H. Lu, W. Yang, J. Zhou and K. Cen, Transcriptome-based analysis on carbon metabolism of *Haematococcus pluvialis* mutant under 15% $CO_2$, *Bioresour. Technol.*, 2017, **233**, 313–321.

64 A. A. Lomeu, O. B. de Oliveira Moreira, M. A. L. de Oliveira and H. V. de Mendonca, Applying ozone in cattle wastewater to maximize lipid production in microalgae biomass, *Bioenergy Res.*, 2023, **16**, 2489–2501.

65 A. J. Simkin, P. E. López-Calcagno and C. A. Raines, Feeding the world: improving photosynthetic efficiency for sustainable crop production, *J. Exp. Bot.*, 2019, **70**, 1119–1140.

66 H. Peng, J. Fu, Y. Huang, *et al.*, Deciphering mechanism of sulfide stress on microalgae and overcoming its inhibition by regulation growth acclimatization period, *Chem. Eng. J.*, 2024, **495**, 153045.

67 P. R. Yaashilaa, A. Saravanan, P. S. Kumar, *et al.*, Role of microbial carbon capture cells in carbon sequestration and energy generation during wastewater treatment: a sustainable solution for cleaner environment, *J. Environ. Manage.*, 2024, **52**, 799–820.

68 A. Guldhe, V. Bhola, I. Rawat and F. Bux, Carbon Dioxide Sequestration by Microalgae: Biorefinery Approach for Clean Energy and Environment, *Bioresour. Technol.*, 2015, **7**, 147–154.

69 E. Daneshvar, R. J. Wicker, P. L. Show and A. Bhatnagar, Biologically-mediated carbon capture and utilization by microalgae towards sustainable $CO_2$ biofixation and biomass valorization – a review, *Sci. Total Environ.*, 2022, **427**, 130884.